Evaluation of column performance in constant pressure and constant flow capillary gas chromatography

Leonid M. Blumberg[a],*, William H. Wilson[b], Matthew S. Klee[b]

[a]*Fast GC Consulting, P. O. Box 585, Hockessin, DE 19707, USA*
[b]*Hewlett-Packard Co., 2850 Centerville Rd., Wilmington, DE 19808, USA*

Abstract

It has been demonstrated that there is no significant difference between the maximum peak capacity and analysis time at the same peak capacity in constant pressure (isobaric) and constant flow (isorheic) modes of temperature programmed GC. In view of that, the choice between the two pneumatic modes should be based on considerations other than the speed-separation performance of the column. © 1999 Elsevier Science B.V. All rights reserved.

Keywords: Column performance; Peak capacity; Temperature programming; Constant pressure; Constant flow

1. Introduction

With the recent introduction of electronic pneumatic control (EPC) in commercial GC (gas chromatography) instruments, maintaining constant flow-rate of a carrier gas (*constant flow or isorheic* [1] *mode*) during a temperature programmed analysis became as easily accessible as maintaining constant head pressure on the column (*constant pressure or isobaric mode*). Theoretical evaluation [1–3] and practical applications (see reviews in Refs. [4–6]) of the constant flow mode were discussed in the literature before. However, no comprehensive theory capable of predicting column performance in the constant flow mode of a temperature programmed GC has been published. Also, the target of the published applications was to achieve certain practical results, but not to expose the mechanisms under-

lying the performance of the technique. As a result, the expectations for the comparative performance of the two pneumatic modes – constant pressure and constant flow – were unclear, and, some times, controversial [7,8].

Here we provide experimental data demonstrating that there is no significant difference between the speed-separation capabilities of a capillary column in either of the two pneumatic modes of a temperature programmed analysis. While not offering a cohesive theory capable of predicting this result, we attempt to explain the outcome. This helped us to better understand the mechanisms underlying the comparative column performance in each pneumatic mode. We hope that the readers can also find this material useful.

2. Nomenclature

The symbols used in the study are compiled in

*Corresponding author – an employee of Hewlett-Packard Co. until November 1998.

Table 1
Symbols

Symbol	Description
A	Internal cross-section area of a column
D_m	Diffusion coefficient of a solute in a gas
$D_{m,e}$	Diffusion coefficient of an eluting solute
$D_{m,r}$	Reference diffusion coefficient of a solute in a gas
D_s	Diffusion coefficient of a solute in a stationary phase
d_s	Stationary phase film thickness
F	Carrier gas flow-rate at reference pressure (typically 1 atm), and temperature (typically, 0°C or 25°C)
f	Carrier gas flow-rate at local pressure and temperature along the column
f_o	Carrier gas flow-rate at the column outlet pressure and temperature
F_{opt}	Optimum F
g	Giddings' compressibility factor ($1 \leq g \leq 9/8$)
H	Column plate height
H_{min}	Minimum plate height
k	Solute retention factor
L	Column length
mln	Milliliter of gas at normal conditions (1 atm, 25°C)
mls	Milliliter of gas at standard conditions (1 atm, 0°C)
n	Column plate capacity
p	Local pressure in a column
p_i	Column inlet pressure
p_o	Column outlet pressure
p_r	Reference pressure (typically, 1 atm)
T_c	Column temperature
T_n	25°C (normal ambient temperature)
T_r	Reference temperature (typically, 0°C or 25°C)
T_s	0°C (standard reference temperature)
u	Local velocity of carrier gas
u_o	Outlet velocity of carrier gas
$u_{o,opt}$	Optimum outlet velocity of carrier gas
$\bar{u}$	Average velocity of carrier gas
x	Distance from the column inlet
η	Carrier gas viscosity

Table 1. Even though some temperatures in the table and in the text are shown in degrees Celsius, degrees Kelvin are always assumed in all mathematical expressions below.

3. Theory

In this section, we rearrange and simplify some known chromatographic expressions to make them more useful for the coming discussion of the experimental results.

3.1. Carrier gas flow-rate

It is widely accepted in GC to express a carrier gas

flow-rate – the rate of the transfer of the amount of the carrier gas through the column – in units of the gas volume per unit of time. This is known as a *volumetric* flow-rate. Unfortunately, the value of the volumetric flow-rate depends on the measurement conditions. This can be a source of controversy [7].

Consider a cylindrical column with the uniform *cross-sectional area*,

$$A = \pi d_c^2/4 \qquad (1)$$

where d_c is *internal diameter* of the column.

A *local* volumetric flow-rate, f – the volume of a gas transferred per unit of time through a cross-section located at some distance x from the column inlet – can be expressed as

$$f = Au \tag{2}$$

where u is a *cross-sectional average* of the carrier gas *velocity* at a coordinate x. As the gas pressure changes along the column, so does its local velocity, u, and its flow-rate, f. The change in f follows directly from Eq. (2). This change makes f an inconvenient measure of the flow-rate in a column as a whole. This can be corrected by adopting a convention to measure the flow-rate at a certain coordinate such as the column outlet. Eq. (2) can be written as

$$f_o = Au_o \tag{3}$$

where f_o and u_o are, respectively, *outlet flow-rate* and *outlet velocity* of the carrier gas. While the outlet flow-rate, f_o, is less ambiguous than the flow-rate, f, at an arbitrary point along the column, the measurement of f_o is impractical in many cases. For example, when the column outlet is at vacuum, such as in GC–mass spectrometry (MS), f_o approaches infinity.

To avoid the problem with the measurement of outlet flow-rate at vacuum, and at other special conditions, we shall notice that, for an ideal gas, in a column with a uniform cross-sectional area, the product pu, where p is gas pressure at coordinate x, is independent of x [9]. That allows us to write

$$pu = p_o u_o \tag{4}$$

where p_o is outlet pressure. Eq. (4) suggests that the volumetric flow-rate of a column can be measured by an external flow meter at some fixed a priori known *reference pressure*, p_r, (typically, 1 atm = 101325 Pa).

The use of the external flow meter (as a real device, or as a concept) brings another uncertainty. The gas volume, and, therefore, its volumetric flow-rate, also depends on the gas temperature thus causing another source of ambiguity in expressing the volumetric flow-rate. To avoid that ambiguity, the flow-rate can be measured at a fixed a priori known *reference temperature*, T_r, (typically 0°C or 25°C), and pressure. So described, the volumetric flow-rate, F, of an ideal gas can be expressed via the outlet flow-rate, f_o, as

$$F = f_o p_o T_r / (p_r T_c) \tag{5}$$

where T_c is the column temperature.

Speaking of the column flow-rate in the following text, we will always assume the quantity, F, described in Eq. (5), unless otherwise is explicitly stated. For a given carrier gas, this quantity is proportional to *mass flow-rate*, *mole flow-rate*, and other similar measures [10] of the rate of the transfer of the gas.

The certainty of the flow-rate, F, described in Eq. (5) depends on the certainty of the reference pressure, p_r, and temperature, T_r.

Following the widely accepted convention, we will always assume – unless otherwise explicitly stated – that

$$p_r = 1 \text{ atm} \tag{6}$$

Unfortunately, the choice for the reference temperatures, T_r is less unique. Two conventions are widely used:

$$T_r = T_s = 0°C \text{ (standard temperature)} \tag{7}$$

$$T_r = T_n = 25°C \text{ (normal ambient temperature)} \tag{8}$$

Typically, the gas flow-rate in GC is measured in units of ml/min (milliliters per minute), regardless of the measurement conditions. To further avoid confusion, we will refer to the gas volume of one milliliter measured at 1 atm and the standard temperature of 0°C as to the *standard milliliter*, abbreviated as mls. The respective unit of gas flow-rate, measured at 1 atm and 0°C becomes mls/min[1]. Similarly, the volume of one milliliter measured at 1 atm and the normal temperature of 25°C can be referred to as a *normal milliliter*, abbreviated as mln. The respective unit of gas flow-rate, measured at 1 atm and 25°C becomes mln/min.

To express the gas flow-rate in Eq. (5) via its outlet velocity and column dimensions, Eqs. (1) and (3) can be used. Combining them with Eq. (5), one has

$$F = \frac{\pi d_c^2 u_o p_o T_r}{4 p_r T_c} \tag{9}$$

According to Darcy's law [11], u_o can be found as

---

[1]This unit is also known as sccm (standard cubic centimeters per minute).

$$u_o = \frac{d_c^2(p_i^2 - p_o^2)}{64 L p_o \eta} \qquad (10)$$

yielding

$$F = \frac{\pi d_c^4 (p_i^2 - p_o^2) T_r}{256 L p_r \eta T_c} \qquad (11)$$

where L is the column *length*, p_i is the *inlet pressure* in the column and η is the carrier gas *viscosity*.

The gas viscosity is almost independent of pressure and, for the common types of carrier gas, changes with the temperature approximately as [12,13] $\eta = \eta_r (T_c / T_r)^{0.7}$, where η_r is the viscosity at T_r. Eq. (11) becomes:

$$F = \frac{\pi d_c^4 (p_i^2 - p_o^2)}{256 L p_r \eta_r} \left(\frac{T_c}{T_r} \right)^{-1.7} \qquad (12)$$

3.2. Simplified expressions for column plate height

The rate of the broadening of the solute zones migrating in the column can be described by *plate height, H*. The latter can be expressed as [14,15]

$$H = g \cdot \left(\frac{B}{u_o} + C_1 u_o \right) + C_2 \bar{u} \qquad (13)$$

where $\bar{u}$ is the *average* velocity of the carrier gas, and

$$B = 2 D_m, \quad C_1 = \frac{(1 + 6k + 11k^2) d_c^2}{96(1+k)^2 D_m},$$

$$C_2 = \frac{2 k d_s^2}{3(1+k)^2 D_s} \qquad (14)$$

where D_m is the *diffusion coefficient* of a solute in the carrier gas, D_s is the *diffusion coefficient* of a solute in the stationary phase, d_s is the stationary phase *film thickness*, g is the gas *compressibility factor* that monotonically changes from 1 at low pressure drop to 9/8 – at high pressure drop and k is the solute *retention factor*.

Coefficients C_1, C_2, in Eq. (14), contain too many unnecessary details for our study. Ignoring these details helps to substantially simplify the forthcoming discussion. To do so, we notice first that, in the majority of practically important cases, the contribution of the stationary phase film thickness to the column plate height is minor and, therefore, can be

ignored. This is especially true [16] for the analyses of complex mixtures where majority of the solutes migrate through the major portion of the column with the retention factors, k, substantially larger that 0.5. This allows one to assume without a substantial error that

$$C_2 = 0 \qquad (15)$$

Furthermore, for the large k values, quantity

$$G(k) = \frac{(1 + 6k + 11k^2)}{96(1+k)^2} \qquad (16)$$

in C_1 becomes nearly constant gradually approaching its maximum at $11/96 \approx 0.115$, Fig. 1. It is convenient to replace $G(k)$ for the large values of k with $1/9$, i.e., to assume that

$$G(k) \approx 1/9 \qquad (17)$$

Eq. (13) becomes

$$H = \left(\frac{2 D_m}{u_o} + \frac{d_c^2 u_o}{9 D_m} \right) g \qquad (18)$$

For the optimum outlet velocity, $u_{o,opt}$, corresponding to the minimum plate height, H_{min}, and, eventually, to the maximum column efficiency and peak capacity [15,17,18], this relation gives

$$u_{o,opt} = \frac{3 \sqrt{2} D_m}{d_c}, \quad H_{min} = g \frac{2 \sqrt{2} d_c}{3} \approx d_c \qquad (19)$$

Due to Eq. (9), optimum flow-rate, F_{opt}, can be found as

$$F_{opt} = \frac{3 \pi D_m d_c p_o}{\sqrt{8} p_r} \left(\frac{T_c}{T_r} \right)^{-1} \qquad (20)$$

One can verify by direct substitution of Eq. (19) in Eq. (18) that the latter can be expressed via symmetric forms

$$H = \frac{1}{2} \left(\frac{u_{o,opt}}{u_o} + \frac{u_o}{u_{o,opt}} \right) H_{min}$$

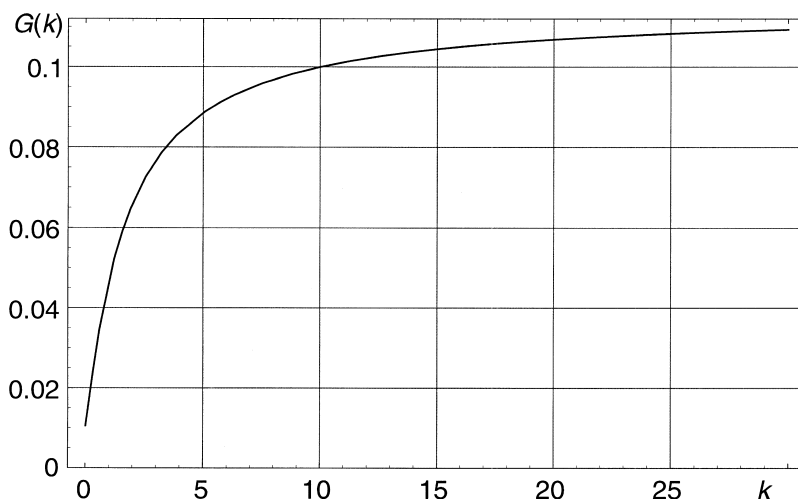$$= \frac{1}{2} \left(\frac{F_{opt}}{F} + \frac{F}{F_{opt}} \right) H_{min} \qquad (21)$$

Fig. 1. Graph of function $G(k)$, Eq. (16).

4. Experimental

In all tests, a HP 6890 GC system equipped with EPC and HP 7673 autosampler was used. The test method included a 30 m × 320 μm × 0.25 μm HP 5 column, a single ramp oven temperature program from 50°C to 320°C with no initial temperature plateau, and an FID (flame ionization detector) system. A test mixture of normal hydrocarbons (C_{10}, C_{12}, C_{14}, C_{16}, C_{18}, C_{20}, C_{22}, C_{23}, C_{24}, C_{26}, C_{28}, C_{30}, C_{32}, C_{36}, C_{40}) was injected using a split ratio 50:1. Helium and hydrogen were used as carrier gases. Oven temperature ramp rate was 5°C/min with helium, and 7.07°C/min with hydrogen. The latter value resulted from using GC method translation software [19] to translate a helium method to a hydrogen method. In constant pressure mode, several pressure setpoints between 5 p.s.i. and 25 p.s.i. were used (1 p.s.i. = 6894.76 Pa). In constant flow mode, several flow-rate setpoints between 0.5 mln/min and 10 mln/min were used.

4.1. Designing the experiments

The following guidelines were used in designing the experiments to compare the speed-separation performance of constant flow and constant pressure modes in a temperature programmed GC.

To reduce the number of variables in the tests, a single ramp temperature program with no initial temperature plateau was used.

For a fixed temperature program, resolution of some critical pairs can be sensitive [20] to changes in void time. In the two pneumatic modes, the void time changes during the run in a different way. As a result, one can see substantial differences in the resolution of some critical pairs when comparing the two modes. Some critical pairs that were well resolved in one pneumatic mode can become unresolved or even switch elution order in the other mode. However, there is no reason to expect that one mode has a fundamental advantage over the other in that respect. Therefore, it was decided to run the tests with a mixture of normal hydrocarbons, and judge the resolving power of each analysis by its peak capacity [15,17,18] rather than by the resolution between the individual peaks. The peak capacity for each set of conditions was calculated as a sum of all resolutions between the neighboring peaks from the first to the last peak eluting during the temperature ramp.

We expected that the results received for one type of carrier gas should allow for a straightforward prediction of the results for a different carrier gas. To verify that, we used helium and hydrogen. Several constant pressure and constant flow runs with differ-

ent pressure (in constant pressure mode) and different flow-rates (in constant flow mode) were made for each gas.

It was further expected that the difference, if any, between the two pneumatic modes would be better exposed in a wide temperature program range. In a single ramp temperature program from 50°C to 320°C, C_{30} was the last in our C_{10}–C_{40} test mixture to elute before the 320°C temperature was reached in all tests. Depending on pressure or flow-rate in each particular test, elution temperature of C_{30} was near 300°C. Retention time of C_{30} was used as a measure of the speed of analysis.

The ramp rate was selected to be close to 10°C per void time [21–23] at initial temperature and efficiency-optimized gas flow-rate [24–26]. For helium at 50°C and flow-rate of 1.5 mln/min, the void time is about 2 min. At 10°C per void time, this corresponds to about 5°C/min. The 7.07°C/min ramp rate for hydrogen is a translation [21,27,28] of the helium 5°C/min ramp determined using GC method translation software [19].

5. Results and discussion

In the following discussion, we assume that, in the *constant pressure mode*, both inlet and outlet pressure on the column remain constant during the temperature programmed analysis. The *constant flow mode* assumes that the rate of transfer of the amount of carrier gas through the column remains constant during the temperature programmed analysis. In all discussions below, this rate is expressed in units of mln/min (normal milliliters per minute, see Theory), i.e., in the units where the volume of gas is measured at *normal* conditions of 1 atm and 25°C regardless of the actual column temperature and outlet pressure.

5.1. General observations

Four chromatograms yielding the highest or near highest peak capacity – two for helium and two for hydrogen with one of each at constant pressure and constant flow mode – are shown in Fig. 2. The graphs of the peak capacities calculated as the sums of all resolutions between the neighboring peaks in each run, and the analysis times (retention times of C_{30}) vs. pressure or flow-rate setpoints are shown in Fig. 3.

We believe that the errors of all subsequent estimations based on the values of peak capacities and their maxima stay within the accuracy of the measurement of the peak capacities and locating their maxima.

Fig. 3 shows that, as expected, the run time monotonically declines with the increase of pressure or flow-rate. However, the peak capacity, as a function of pressure or flow-rate, has a clear maximum.

As the temperature programs for helium and hydrogen are mutual translations of each other, we expected that the speed gain due to the use of hydrogen instead of helium should be about 41% in each pneumatic mode. The experimental data show that, at the maximum peak capacity, the analysis lasted for helium about 40.2% longer than for hydrogen in the constant pressure mode, and 42.7% longer in the constant flow mode.

Fig. 3 also shows that the maximum peak capacity is independent of both the carrier gas type and the pneumatic mode. All four maxima in peak capacity are confined within ±2% spread – between 552 for hydrogen at 2 mln/min and 575 for helium at 10 p.s.i. The independence of these maxima on the gas type was expected because, in each pneumatic mode, the method with hydrogen was a translation of the method with helium.

What is more interesting, however, is that, for a given carrier gas, the maximum peak capacity and the analysis time at that maximum is almost the same regardless of the pneumatic mode. (Notice however, that the initial pressure for the optimal constant flow mode is lower than that for the optimal constant pressure mode). From the constant flow to the constant pressure mode, analysis time only slightly increases from 46.432 min to 47.280 min for helium, and from 32.525 min to 33.732 min for hydrogen. The difference is less than 4%. This is hardly significant in practice, and falls within the experimental errors of these experiments.

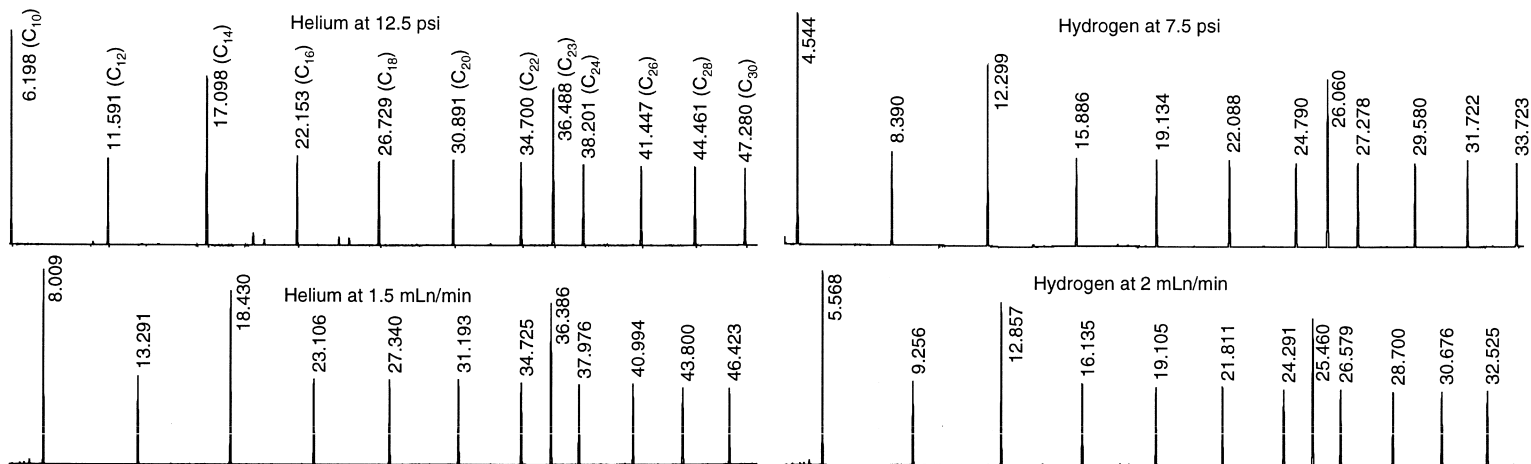We can conclude that, at least within the scope of our experiments

Fig. 2. Examples of constant pressure (upper row) and constant flow (lower row) normal hydrocarbon chromatograms with helium at 5°C/min and hydrogen at 7.07°C/min – both from 50°C with no initial plateau.
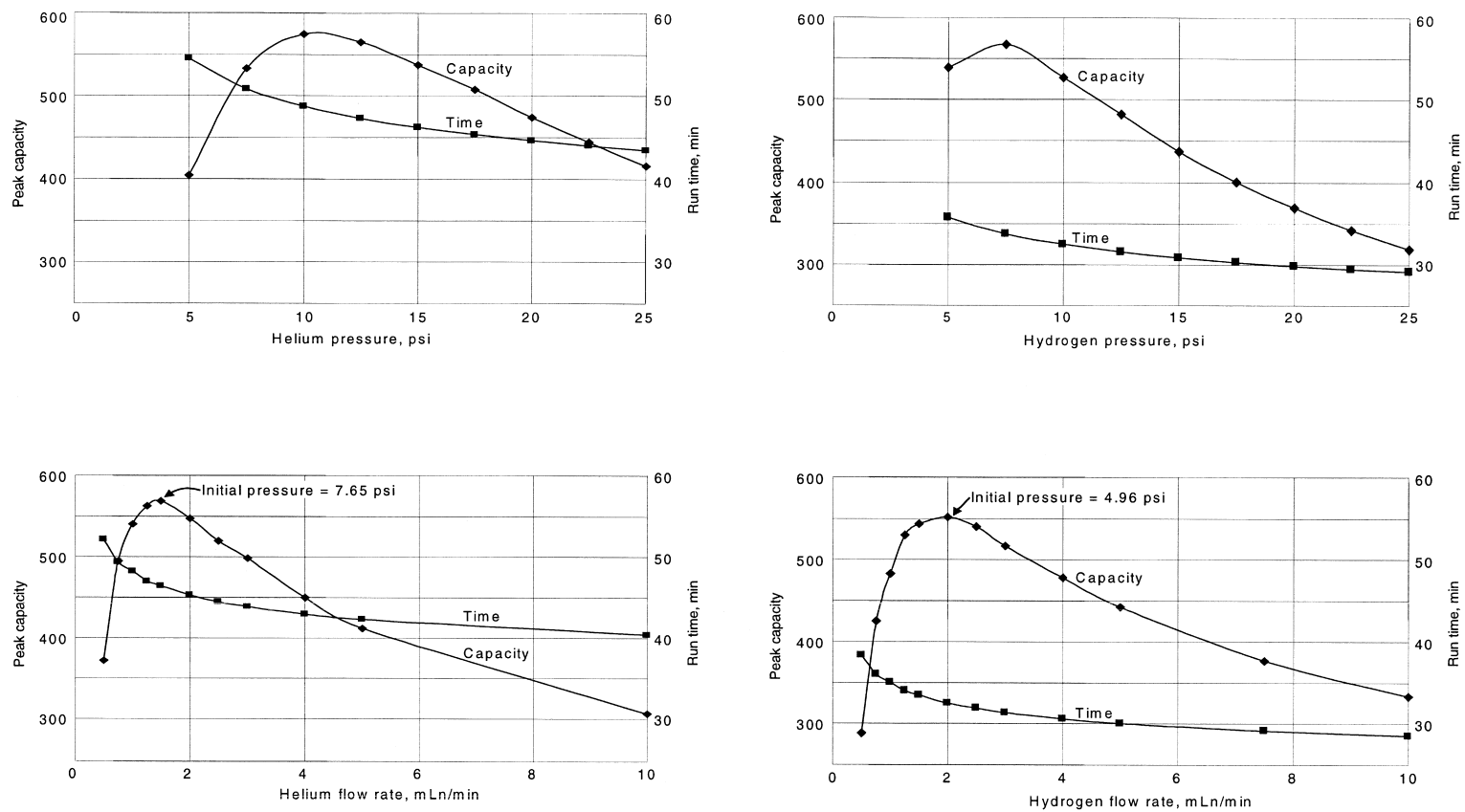
Fig. 3. Peak capacity and run time for helium at 5°C/min and hydrogen at 7.07°C/min vs. flow-rate (in constant flow mode) and head pressure (in constant pressure mode).

Nearly the same peak capacity can be achieved in nearly the same time in both pneumatic modes of a temperature programmed analysis

This conclusion coincides with the previous estimates [8]. Without offering a comprehensive theory capable of predicting this conclusion, we explain it as follows.

5.2. Peak capacity

First of all, observing chromatograms in Fig. 2 we can reasonably assume that all peaks are well retained. The earliest peak in all chromatograms is C_{10}, eluting at 4.544 min in the chromatogram for hydrogen at 7.5 p.s.i. At the temperature ramp rate of 7.07°C/min, this corresponds to elution temperature of about 82°C. The void time at this temperature is about 0.93 min suggesting the apparent retention factor, k, of about 4. During the migration of C_{10} through the column, the column temperature changes by approximately 30°C. Published estimates [22,23,29,30] suggest that a 30°C temperature change changes k by about a factor of 2, from the value that is larger that 4 at the beginning of the run to the value that is slightly lower than 4 when it elutes. Other peaks in the same chromatogram start with much higher k values.

Secondly, the column has a reasonably thin film whose contribution to the plate height can be ignored.

With these simplifying assumptions, column plate height can be described by Eq. (18) yielding a simple formula, Eq. (20), for the optimum flow-rate, F_{opt}, that corresponds to the minimum plate height, and, eventually, – to the maximum peak capacity. According to Eq. (20), F_{opt} in a temperature programmed analysis should change in proportion with the quantity D_m/T_c where D_m is the diffusion coefficient of a solute in the carrier gas and T_c is the absolute temperature of the column.

For a given solute, D_m can be described [31] as

$$D_m = D_{m,r} (T_c/T_r)^{1.75} \qquad (22)$$

where $D_{m,r}$ is D_m at the reference temperature, T_r is always 298.15 K in this discussion. The reference diffusion coefficient, $D_{m,r}$, in Eq. (22) generally declines with the increase in the solute molecular mass.

At any given time, many solutes migrate through the column. Due to the difference in their $D_{m,r}$ values in Eq. (22), the solutes can have different diffusion coefficients, and, therefore, can have different optimum gas flow-rates. Because of that, there can be no single flow-rate value that is the best for all solutes at any given time. On the positive side, however, is the fact that, by any given time in a temperature programmed analysis, some solutes – typically, the lightest – might have already eluted from the column, while others – typically, the heaviest – might still just have barely moved from the inlet area due to their high retention at the still not sufficiently high column temperature. This suggests that, at any given time in a temperature programmed analysis, only a part of the solutes having somewhat similar molecular masses actively migrate through the column. In this discussion, we will use the diffusion coefficient, $D_{m,e}$, of a solute eluting[2] at temperature T_c as the diffusion coefficient of the entire actively migrating group of the solutes at T_c.

The molecular masses of the eluting solutes increase with temperature in a temperature programmed analysis. As a result, quantity $D_{m,r}$ in Eq. (22) declines with the increase in T_c. Therefore, the net rate of change in $D_{m,e}$ as a function of T_c for the eluting solutes should be lower than $T_c^{1.75}$ in Eq. (22) for a single solute. The plots of $D_{m,e}$ vs. T_c for the eluting peaks in the chromatograms in Fig. 2 are shown in Fig. 4. Equations from Refs. [31,32] were used for the calculation of $D_{m,e}$.

The plots in Fig. 4 show that, the diffusion coefficient, $D_{m,e}$, of the eluting hydrocarbons in chromatograms of Fig. 2, can be approximated as

$$D_{m,e} \approx 0.256(T_c/T_r)^{0.4} \ (\text{cm}^2/\text{s}), \text{ for helium} \qquad (23)$$

and

$$D_{m,e} \approx 0.321(T_c/T_r)^{0.4} \ (\text{cm}^2/\text{s}), \text{ for hydrogen} \qquad (24)$$

---

[2]Giddings [22] has shown that *significant temperature* – about T_c – 40 K – is more appropriate for these type of evaluations. However, this correction is not essential to our analysis.
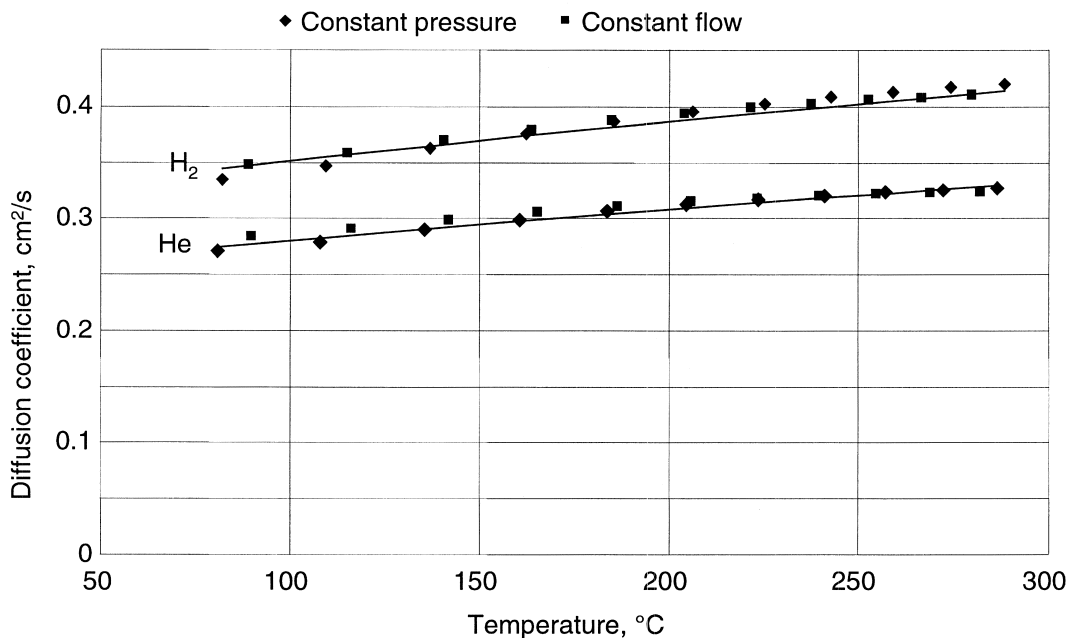
Fig. 4. Diffusion coefficients, of C_{10} through C_{30} vs. their elution temperature in chromatograms of Fig. 2. Solid lines are approximations in Eqs. (23) and (24).

Eqs. (23) and (24) indicate that, in all four chromatograms or Fig. 4,

$$D_{m,e} \sim T_c^{0.4} \qquad (25)$$

It can be verified that this approximation remains satisfactory for all chromatograms in this series of tests. Furthermore, there are the reasons to expect that Eq. (25) accommodates a broad range of mixtures and *normal* temperature ramp rates (in vicinity of 10°C per void time).

The proportion in Eq. (25) suggests that, when the column temperature, T_c, increases, the optimum flow-rate, F_{opt}, that is proportional to $D_{m,e}/T_c$, according to Eq. (20), declines in proportion with about $T_c^{-0.6}$, i.e., Fig. 5,

$$F_{opt} \sim D_{m,e}/T_c \sim T_c^{0.4}/T_c \sim T_c^{-0.6} \qquad (26)$$

This means that,

For the highest peak capacity, the flow-rate in a temperature programmed run should decline in proportion with about $T_c^{-0.6}$

What actually takes place in the Fig. 2 chromatograms?

In the constant pressure mode, the flow-rate declines, according to Eq. (12), in proportion with about $T_c^{-1.7}$, i.e., Fig. 5,

$$\text{at constant pressure, } F \sim T_c^{-1.7} \qquad (27)$$

This decline in actual F is about $T_c^{1.1}$ steeper than optimum. One can express it as, Fig. 5,

$$\text{at constant pressure, } \frac{F}{F_{opt}} \sim \frac{T^{-17}}{T^{-0.6}} \sim T_c^{-1.1} \qquad (28)$$

In the constant flow mode, on the other hand, Eq. (26) yields, Fig. 5, in view of $F=$ constant,

$$\text{at constant flow, } \frac{F}{F_{opt}} \sim T_c^{0.6} \qquad (29)$$

As the actual flow-rate remains constant while a decline is needed for maximum peak capacity, quantity $T_c^{0.6}$ in Eq. (29) can be viewed as the measure of the lack of the flow-rate decline.
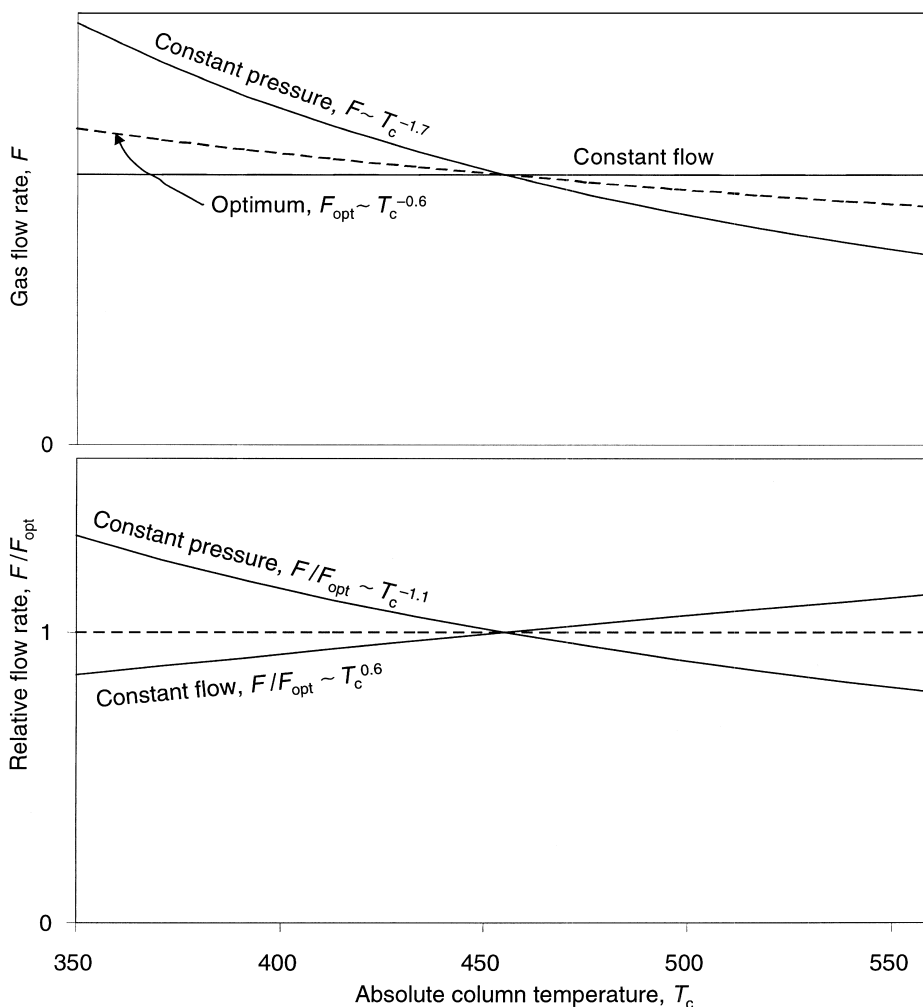
Fig. 5. Gas flow-rate, F, (absolute, upper graphs), and the same in relation to the optimum flow-rate, F_{opt}, (lower graphs) vs. column temperature, T_c.

These evaluations can be summarized, Fig. 5, as follows. Eqs. (28) and (29) describe the mismatch between the changes in the optimum flow-rate, F_{opt}, and the actual flow-rates, F, in the two pneumatic modes. The mismatch lowers the peak capacity compared to the available maximum for a given temperature program. According to Eq. (26), in order to achieve the maximum peak capacity, F should decline in proportion with $T_c^{-0.6}$. Actually, in the constant pressure mode, F declines in proportion with $T_c^{-1.7}$, i.e., $T_c^{1.1}$ steeper than it is necessary for the maximum peak capacity. On the other hand, the fact that flow-rate does not decline at all in the

constant flow mode, causes the lack of the decline in F that increases in proportion with $T_c^{0.6}$. The bottom line is that

In both pneumatic modes, there is a gradually changing mismatch between the optimal and the actual flow-rate of carrier gas

As the mismatch in the constant pressure mode changes more rapidly than that in the constant flow mode, we will concentrate our further attention on the former.

It is very likely that, at the maximum peak

capacity in the constant pressure mode, the actual flow-rate, F, that declines more rapidly than needed, is higher than F_{opt} at the beginning of the analysis, and lower than F_{opt} at the end. For example, in case of helium at 12.5 p.s.i., C_{10} (the first peak) elutes at about 81°C or 354 K while C_{30} (the last) – at about 286°C or 559 K. In this temperature range, the flow-rate drops from 2.4 mln/min to 1.1 mln/min (*normal* ml/min, see Theory for explanation).

Let us assume for the sake of simplicity that the flow-rate is optimal somewhere in the middle of the temperature range, i.e., at about 450 K (177°C). That means, according to Eq. (28), that C_{10} elutes when

$$F/F_{opt} \approx (354\,\text{K}/450\,\text{K})^{-1.1} \approx 1.3$$

(i.e., the actual flow-rate is 30% above its optimum). At the time of elution of C_{30}, on the other hand,

$$F/F_{opt} \approx (559\,\text{K}/450\,\text{K})^{-1.1} \approx 0.79$$

(i.e., the actual flow-rate is 21% below its optimum). The largest 1.3 time mismatch between the actual and the optimum flow-rates at the beginning of analysis can lead, according to Eq. (21), to up to

$(1.3 + 1/1.3)/2 \approx 1.035$, (i.e., up to 3.5%) increase in the column plate height, H. This, due to the proportionality [15]

$$n \sim 1/\sqrt{H}$$

means about 1.7% loss in the peak capacity, n. As the gas flow-rate changes from being above its optimum level at the beginning of the run to ending below its optimum, the net loss in the peak capacity through the entire run should be lower than the 1.7% worst case loss. This loss is certainly not very significant in practice.

The peak capacity loss in the constant flow mode is expected to be even smaller. It is interesting in this regard that the resolution between the neighboring peak pairs is nearly identical in both modes, Fig. 6.

One can conclude that

While the peak capacity achievable at constant pressure or constant flow, is lower compared to the maximum achievable for a given temperature program at the best pneumatic conditions, the deficiency is practically insignificant
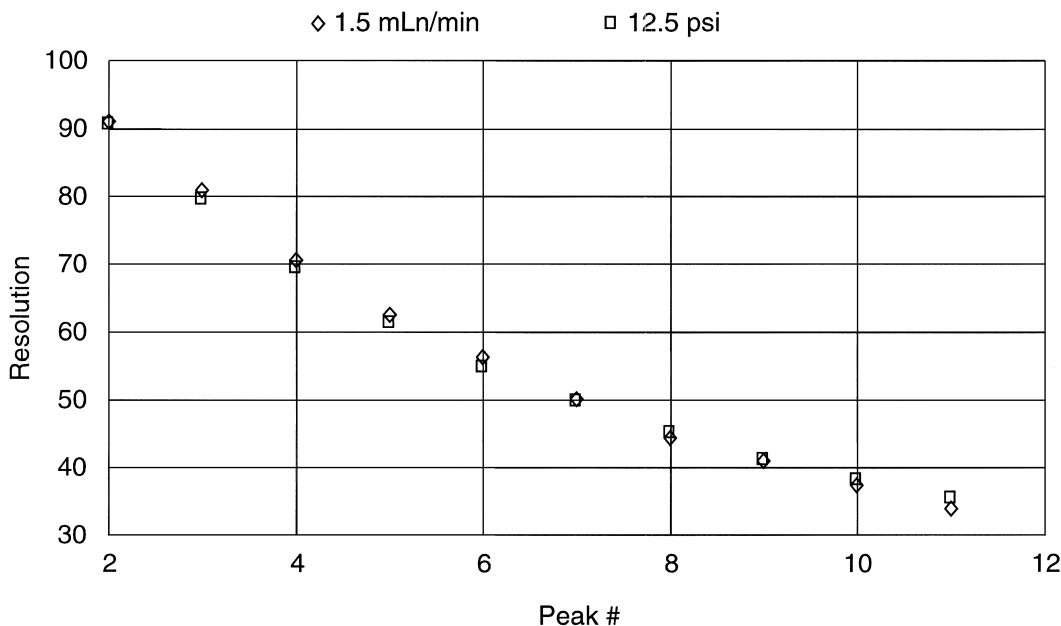
◇ 1.5 mLn/min   □ 12.5 psi

Fig. 6. Resolution between a peak and its predecessor (excluding C_{23}) for helium chromatograms in Fig. 2.

As a result,

> *Nearly the same peak capacity can be achieved in both constant pressure and constant flow modes*

This suggests that the choice between the constant pressure and constant flow modes should be based on the considerations other than the column chromatographic performance. Thus it can be taken into account that the constant flow mode might be preferable for mass spectrometers, and for other detectors. The constant pressure mode, on the other hand, is more suitable [21] for scalable methods that, via GC method translation [19,27,28], can be later adopted to different columns, carrier gas types, detectors, etc., without the change in the peak elution pattern.

Finally, it is worth mentioning that the results established here should not depend upon whether the column pressure drop is low or high, as might be required for fast analyses of complex mixtures. Indeed, the value of the optimum flow-rate, F_{opt}, in Eq. (20) depends (through the gas viscosity) on the column temperature, but not on the pressure drop. Therefore, the mismatch between the constant flow-rate and the temperature dependent F_{opt} in constant flow mode does not depend on the column pressure. Similarly, in the constant pressure mode, although actual flow-rate, F, does change with the column temperature, the change caused by the change in the gas viscosity is the same regardless of the column pressure drop. And so is the mismatch between F and F_{opt}.

5.3. Analysis time

Experimental data for helium and hydrogen as a carrier gas, Figs. 2 and 3, respectively, suggest that, although a slightly shorter analysis time can be observed for the constant flow mode for both gases,

> *There is no significant difference in the analysis time between the two modes when run at their highest peak capacity*

This finding can be explained as follows.
Notice, for example, that for helium in the con-

stant flow mode, Fig. 3, the highest peak capacity is achieved at 1.5 mln/min. Almost the same peak capacity and analysis time in the constant pressure mode, can be achieved at 12.5 p.s.i. where the flow-rate changes from 2.8 mln/min at the beginning of the run to 1.1 mln/min at the elution of the last peak. In other words, at the beginning of the constant pressure analysis, its flow-rate is about 1.9-times higher compared to that in the constant flow mode. On the other hand, at the time of elution of the last peak in the constant pressure mode, the flow-rate is about 1.4-times lower compared to that in the constant flow mode. This equilibrates the analysis times in both modes.

The same evaluation can be applied to the data for hydrogen which represent merely the scaled version of the data for helium.

More detailed analysis might require a careful accounting for the compressibility of the carrier gas. This is out of the scope of this report. However, it is worth mentioning that the high pressure drop required for the fast analysis of complex mixtures should not alter the small difference between the speed of analyses in the two pneumatic modes. In fact, the difference, if any, between the analysis time at the same peak capacity in the constant flow and the constant pressure modes should decline with the increase of the column pressure. Indeed, as we established earlier, due to the temperature induced increase in the gas viscosity, the gas flow-rate gradually declines in a constant pressure temperature programmed analysis. So does the gas velocity, causing reduction in the speed of separation toward the end of analysis. The degree of these viscosity caused changes in a constant pressure mode are the same regardless of the column pressure level. Things are different in the constant flow mode. To maintain the constant flow-rate at the increasing temperature, the column pressure drop must increase. At the low pressure drop, the effect is minor so that gas velocity remains nearly the same during the entire run. When the column pressure drop is high, however, its further increase during the run causes further compression of the gas. That, in turn, causes gradual reduction in the gas's average velocity with time, although the flow-rate remains constant. This decline in the gas velocity with time in the constant flow mode makes this mode more similar to the constant

pressure mode than in the low pressure drop case, further diminishing the already small difference in the speed characteristics of the two modes.

6. Conclusion

There is almost no difference in the speed-separation performance of a capillary column between constant pressure and constant flow modes of temperature programmed GC. Nearly the same maximum peak capacity at nearly the same analysis time can be achieved in both modes. The minor difference between the two modes that has been observed is within the experimental error of the experiments performed.

Considerations other than column performance can be more important for the selection of one of these modes over the other. Among these considerations can be the preference for constant flow-rate in mass spectrometers and other detectors. The constant pressure mode, on the other hand, is more suitable for the creation of translatable methods that result in the same peak elution patter for different columns, different carrier gas types, different detectors, etc. The optimal pressure for constant pressure mode is higher than the initial pressure for constant flow mode.

References

[1] C. Costa Neto, J.T. Köffer, J.W. De Alencar, J. Chromatogr. 15 (1964) 301–313.

[2] A. Zlatkis, D.C. Fenimore, L.S. Ettre, J.E. Purcel, J. Gas Chromatogr. 3 (1965) 75–81.

[3] F.R. Gonzalez, A.M. Nardillo, J. Chromatogr. 757 (1997) 109–118.

[4] S.S. Stafford, K.J. Klein, P.A. Larson, R.L. Firor, P.L. Wylie, Applications of Electronic Pressure Control and Pressure Programming in Capillary Gas Chromatography (43) 5091-2731E, Hewlett-Packard Co., Wilmington, DE, 1991.

[5] M.S. Klee, V. Giarrocco, H. Fatunmbi, R.L. Firor, F. David, in: P. Sandra, G. Devos (Eds.), 16th International Symposium on Capillary Chromatography, Palazzo dei Congressi, Riva del Garda, 27–30 September 1994, Hüthig, Heidelberg, 1994, pp. 135–148.

[6] S.S. Stafford, Electronic Pressure Control in Gas Chromatography, Hewlett-Packard Co, Wilmington, DE, 1994.

[7] K. Grob, J. Chromatogr. 17 (1994) 556.

[8] L.M. Blumberg, T.A. Berger, M.S. Klee, J. High Resolut. Chromatogr. 18 (1995) 378–380.

[9] L.M. Blumberg, Chromatographia 44 (1997) 325–329.

[10] L.M. Blumberg, J. High Resolut. Chromatogr. 22 (1999) 213–216.

[11] G. Guiochon, in: M. Lederer (Ed.), Chromatographic Review, Elsevier, Amsterdam, 1966, pp. 1–47.

[12] Y.S. Touloukian, S.C. Saxena, P. Hestermans, Viscosity, IFI/Plenum Press, New York, 1975.

[13] J.V. Hinshaw, L.S. Ettre, J. High Resol. Chromatogr. 20 (1997) 471–481.

[14] G.H. Stewart, S.L. Seager, J.C. Giddings, Anal. Chem. 31 (1959) 1738.

[15] J.C. Giddings, Unified Separation Science, Wiley, New York, 1991.

[16] L.M. Blumberg, J. High Resolut. Chromatogr. (1999) in press.

[17] J.C. Giddings, Anal. Chem. 39 (1967) 1027–1028.

[18] E. Grushka, Anal. Chem. 42 (1970) 1142–1147.

[19] Hewlett-Packard Co., GC Method Translation [for Windows], Hewlett-Packard Co., Wilmington, DE, 1998.

[20] R.J. Pell, H.L. Gearhart, J. High Resolut. Chromatogr. 10 (1987) 388–391.

[21] L.M. Blumberg, M.S. Klee, Anal. Chem. 70 (1998) 3828–3839.

[22] J.C. Giddings, in: N. Brenner, J.E. Callen, M.D. Weiss (Eds.), Gas Chromatography, 13–16 June 1961, Academic Press, New York, 1962, pp. 57–77.

[23] J.C. Giddings, J. Chem. Educ. 39 (1962) 569–573.

[24] L.M. Blumberg, J. High Resolut. Chromatogr. 20 (1997) 679–687.

[25] L.M. Blumberg, J. High Resolut. Chromatogr. (1998) in press

[26] L.M. Blumberg, M.S. Klee, in: Proceedings of 20th International Symposium on Capillary Chromatography, Palazzo dei Congressi, Riva del Garda, 26–29 May, 1998, I.O.P.M.S, Kortrijk, 1998, CD-ROM.

[27] W.D. Snyder, L.M. Blumberg, in: P. Sandra (Ed.), Proceedings of 14th Intl. Symp. on Capillary Chromatography, Baltimore, 25–29 May, 1992, pp. 28–38.

[28] M.S. Klee, V. Giarrocco, Predictable Translation of Capillary Gas Chromatogr. Methods for Fast GC (23) 5965-7673E, Hewlett-Packard Co., Wilmington, DE, 1997

[29] A.B. Littlewood, Gas Chromatography – Principles, Techniques and Applications, Academic Press, New York, 1970.

[30] M. Goedert, G. Guiochon, Anal. Chem. 42 (1970) 962–968.

[31] E.N. Fuller, J.C. Giddings, J. Gas Chromatogr. 3 (1965) 222–227.

[32] E.N. Fuller, P.D. Schettler, J.C. Giddings, Ind. Eng. Chem. 58 (1966) 19–27.